Theoretical evaluation of the susceptometric measurement of iron in human liver by four different susceptometers

2002 Physiol. Meas. 23 683

(http://iopscience.iop.org/0967-3334/23/4/308)

INSTITUTE OF PHYSICS PUBLISHING PHYSIOLOGICAL MEASUREMENT

Physiol. Meas. **23** (2002) 683–693 PII: S0967-3334(02)39789-2

Theoretical evaluation of the susceptometric measurement of iron in human liver by four different susceptometers

A A O Carneiro[1], O Baffa[1], J P Fernandes[1] and M A Zago[2]

[1] Departamento de Física e Matemática-FFCLRP, Universidade de São Paulo, Av. Bandeirantes, 3900, 14040-901 Ribeirão Preto, SP, Brazil
[2] Fundação Hemocentro de Ribeirão Preto, Universidade de São Paulo, Rua Ten. Catão Roxo, 2501, 14051-140 Ribeirão Preto, SP, Brazil

Received 17 July 2002, in final form 23 August 2002
Published 2 October 2002
Online at stacks.iop.org/PM/23/683

Abstract
This paper is an evaluation of liver iron quantification using a simulated magnetic susceptibility measurement in the hepatic region. Susceptometers having homogeneous and non-homogeneous magnetizing fields coupled with axial second-order and planar first-order gradiometric magnetic detectors were considered. The intensity of magnetic flux threading the detector coils was evaluated considering samples with volume and susceptibility equivalent to liver iron, tissue and lung air individually. These volumes were represented by cylindrical and spherical geometries. The main sources of error in quantifying iron overload in susceptometric measurement of hepatic tissue were evaluated for four configurations of the susceptometer.

Keywords: Susceptibility, iron overload, chronic anaemia, haemochromatosis, ferritin, gradiometer

1. Introduction

Iron accumulation occurs in vital organs such as the heart, liver and endocrine glands. The liver has been the targeted organ to evaluate the excessive iron (as paramagnetic haemosiderin and ferritin) overload because it has a large volume and stores large amounts of the iron present in our body. Iron overload is found in patients with chronic anaemia who are subjected to regular blood transfusion and in patients with hereditary haemochromatosis. Chelation therapy has shown to be quite effective in eliminating the effects of iron toxicity, thus increasing life expectancy. Regular and accurate determination of iron overload is the basis of medical treatment of these patients. Therefore, a non-invasive technique for monitoring iron stores in liver is important to the treatment and follow-up of patients with this condition. The current

standard technique is liver biopsy, which can provide direct measurement of liver iron concentration (LIC) by atomic absorption spectroscopy, and histological evolution of the liver pathology. Unfortunately, the liver biopsy method cannot be used routinely because of its invasiveness, discomfort and significant risk to the patient.

In the last decade, several efforts have been made to find a non-invasive and precise technique to evaluate liver iron overload. Many studies of the interaction of paramagnetic molecules with protons have been realized with nuclear magnetic resonance (NMR) and magnetic resonance imaging (MRI) in an effort to quantify LIC (Baffa *et al* 1986, Kaltvasser *et al* 1990, Gomori *et al* 1991). With fast pulse techniques, shortening of the time to echo (TE) and the increase in the magnetic fields in new MRI systems, some studies have shown good correlation between the transverse relaxation rate (1/T2) and LIC for low levels of iron overload (Engelhardt *et al* 1994, Papakonstantinou *et al* 1995, Clark and St Pierre 2000, Jensen *et al* 1994). Nevertheless, in patients with moderate and severe degree of iron overload the T2 measurement presents poor accuracy (Thomsen *et al* 1992). Another non-invasive technique for the quantification of LIC, which has presented precise results, is the external measurement of magnetic susceptibility (MS) in the liver region using a susceptometer based on the superconducting quantum interference device (SQUID) (Bastuscheck and Williamson 1985, Brittenham *et al* 1982, Paulson *et al* 1990, Carneiro and Baffa 2000). Farrel *et al* (1983) first presented a susceptometric system for accurate assessment of hepatic iron and later Fischer *et al* (1992) showed that the LIC measurement with this susceptometric technique presents a good correlation of LIC measurements by liver biopsy for a range of iron overload from a normal individual (0.1–0.5 mgFe^{3+}/g wet weight) to those in a group of β-thalassemics subjected to regular blood transfusions, where iron concentration can be as high as 30 mgFe^{3+}/g wet weight. The susceptometric technique consists in the measurement of the induced magnetic field produced in the region of the liver in response to an external magnetizing field. The normal biological tissue is diamagnetic and has a magnetic susceptibility close to that of water (-9.032×10^{-6} SI). When atoms of iron are present in the tissue, the increment of the magnetization produced is proportional to the amount of iron present.

In susceptometric measurements of the liver, the iron distributed in this organ, as well as the adjacent tissue (air, skin, fat and bone), contributes to the measurement. Due to the asymmetry and volume variation of this organ and the very small differences among the susceptibility values, it is impossible to determine precisely the susceptometric contribution of each material individually. To minimize the tissue contribution, Farrel *et al* (1980) filled the space between the detector and the subject's torso with water. This way, when the torso is moved away from the detector, the water, having practically the same susceptibility, substitutes for the presence of the tissue and the difference owing to the liver iron is determined. Bastuscheck and Williamson (1985) have used a fixed volume of water on the torso to homogenize the upper surface of it. Improvements in the system's detector coil (Farrel *et al* 1980) and in the magnetizing field system (Della Penna *et al* 1999) reduced the diamagnetic contribution in the susceptometric measurement of the liver. To precisely evaluate the iron concentration from a susceptometric measurement, computer models taking into account the geometry of liver tissue, air, fat, among others, need also to be developed and are treated in this paper.

A critical step in developing a susceptometric system to measure a large sample is the assembling of the magnetizing and the detector coils. The coils must be arranged in a configuration such that the total magnetizing flux in the gradiometer from the external field is practically null. Farrel *et al* (1983) and Paulson *et al* (1990) presented a system in which the magnetizing field is generated by a superconducting coil, with a configuration equivalent to a first-order axial gradiometer, coupled symmetrically with two superconducting second-order axial gradiometer detector coils. The array is positioned inside a vacuum chamber in the dewar.

Bastuscheck and Williamson (1985), Pasquarelli *et al* (1996) and Carneiro and Baffa (2000) presented a susceptometric system with an ac homogeneous magnetizing field generated by a large array of coils not assembled in the same substrate as the detector system. Della Penna *et al* (1999) have studied a susceptometric system with a non-homogeneous magnetizing field, generated by a large coil, with the gradient of the field increasing away from the detector.

In this work, a computational simulation of some details in liver iron quantification using a susceptometric measurement is discussed. Our attention was focused on evaluating the main perturbation compromising the measurement of the LIC and its dependence on the magnetizing coil and detector coil geometry. Four different combinations of susceptometer configurations were simulated with two magnetizing fields (homogeneous and non-homogeneous fields) with two detector coils (second-order axial gradiometer and first-order planar gradiometer). For this, a simplified torso model was used in the computational experiment.

2. Performance of the liver iron susceptometry

The MS measurement of the liver is generally performed with the patient laid down in a supine position below the magnetic detector, with the body rotated 35–40°, leaving the hepatic region as close as possible to the detector. During the measurement this region is magnetized with a known magnetized field and the flux changes threading the detector are registered to different depths of the torso from the pick-up coil.

The response of a magnetic susceptometer is given by the magnetic flux (Φ) threading the detector coil due to the presence of a sample whose susceptibility is being measured. From the reciprocity theorem for susceptometry (Tripp 1983), this flux is represented by the following volume integral:

$$\Phi = \frac{1}{\mu_0 I_d} \int_{\text{vol}} \chi(\vec{r})\, \vec{B}_m(\vec{r}) \cdot \vec{B}_d(\vec{r})\, \mathrm{d}^3 r \tag{1}$$

where $\chi(\vec{r})$ is the magnetic susceptibility of the sample, $\vec{B}_m(\vec{r})$ is the magnetizing flux density and $\vec{B}_d(\vec{r})$ is the magnetic flux density (lead field) that the detector coils would generate in the element of volume ($\mathrm{d}^3 r$) if energized with a current I_d.

3. Torso model and its susceptometric contribution

The sample model used to represent the torso consisted of three independent sub-volumes representing the tissue, liver iron and lung volumes. The geometry and susceptometric contribution attributed to each sub-volume were based on the following considerations: (1) the liver iron was considered homogeneously distributed in a spherical volume with volumetric susceptibility equal to $c_{\text{Fe}}\chi_{m,\text{Fe}}$ where c_{Fe} is the liver iron concentration and $\chi_{m,\text{Fe}}$ is the mass susceptibility of the iron ($\chi_{m,\text{Fe}} = 1.6 \times 10^{-6}$ m^3 kg^{-1} was used). For the adult body, the liver volume is about 1530 cm^3 corresponding to a spherical ray of approximately 7.1 cm; (2) the air in the lungs was considered disturbed in a unique cylindrical volume with length and diameter equal to the liver spherical diameter and the susceptometric contribution derived from this volume was attributed to the presence of air and the absence of tissue, i.e. $\chi_{\text{lung}} = \chi_{\text{air}} - \chi_{\text{tissue}}$ ($\chi_{\text{air}} = 0.36 \times 10^{-6}$ and $\chi_{\text{tissue}} = 9.032 \times 10^{-6}$ (SI) was used); (3) in the absence of liver iron and air into the lungs, the flux changes threading the detector coil should be practically due to the presence of the tissues. In a differential susceptometric measurement, this contribution of the tissue can be practically cancelled by using a water bag between the magnetic detector and the torso of the subject (Farrel *et al* 1983). Nevertheless, in the simulations that follow, the need to use accessories to minimize the tissue contribution was

emphasized. Due to the cylindrical geometry, the adult torso was represented by a cylinder 50 cm in length and 12 cm in diameter and the tissue volume was considered as torso volume minus lung volume.

The perturbation effects from the iron present in the heart and in the spleen as well as the air in the intestine were neglected due to their large distance from the detector. The position of the liver inside a reclining adult torso was considered horizontally symmetrical and at a vertical distance of 1.7 cm from the upper surface of the torso. The distance between the centre of the liver and the boundary of the lung was considered 5 cm. The depth of the lung was considered equal to the liver (1.7 cm from the skin).

According to equation (1) and the torso model described above, the magnetic flux threading the detector coils for the separated contributions derived from liver iron and lung volumes, considering the use of a water bag, can be represented by

$$\Phi_{\mathrm{Fe}} = \frac{c_{\mathrm{Fe}}\chi_{m,\mathrm{Fe}}}{\mu_0}\mathrm{int}_{\mathrm{liver}} \qquad \Phi_{\mathrm{lung}} = \frac{\chi_{\mathrm{air}} - \chi_{\mathrm{tissue}}}{\mu_0}\mathrm{int}_{\mathrm{lung}} \tag{2}$$

where $\mathrm{int}_{\mathrm{vol}}$ is the value of each integral $\int_{\mathrm{vol}} B_m(r)\frac{B_d(r)}{I_d}\,\mathrm{d}r^3$, where 'vol' is each of the three volumes appearing in expression (2). This integral was performed by a summation over small voxels ($0.5 \times 0.5 \times 0.5$ mm^3) and the spatial sensitivity function (SSF) $\left(B_m(r)\frac{B_d(r)}{I_d}\right)$ was obtained for each voxel. The values of fields B_m and B_d in the centre of the voxels were calculated numerically using elliptical integrals (Farrel *et al* 1983).

The relative contribution of each of these substances depends on its magnetic susceptibility, magnetizing coil geometry and detector coil geometry.

4. Features of the simulated susceptometric system

The two different types of detector coils used for each of the simulated susceptometric systems were: (1) a second-order axial gradiometer (SOAG) with a 0.07 m baseline, composed of four identical loops (one loop at each extreme and two in the middle) 0.0254 m (1 inch) in diameter; (2) a first-order planar gradiometer (FOPG) composed of two identical loops 1 cm in diameter and with a 3 cm baseline. These detector coils were combined with two different magnetizing fields: (1) a homogeneous magnetizing field (HMF); (2) a localized magnetizing field (LMF) generated by a small coil, 7 cm in diameter, symmetrically coupled to the detector coil. To guarantee that the LMF on the gradiometers would be null when no sample was present, the magnetizing coil array associated with a SOAG consisted of two identical loops separated by a distance equal to twice the baseline of the gradiometer (14 cm), and the magnetizing coil associated with the FOPG consisted of a unique loop. Figure 1 presents the arrangements of these four simulated susceptometers with their respective equal-sensitivity contour maps associated with the SSF. The contours were mapped in a plane (25×30 cm) that coincides with the axial symmetry axis of the pick-up coil and 1 cm below this coil. The intensity of the contours is equal to $(\vec{B}_m \cdot \vec{B}_d)_{n=1}/n^5$, where n is the number of the contours. Superposed on these contours is also plotted the projection of the cylinders that represent the torso and the lungs and the sphere that represents the liver. The minimum distance between the pick-up coil and the torso was 0.011 m. This distance is equivalent to the gap between the pick-up coil and the tip of the liquid helium dewar. For a homogeneous magnetizing field B_m, the sensitivity of profile $\vec{B}_m \cdot \vec{B}_d$ is proportional to the component of the lead field along the direction of the magnetizing field (figures 1(a) and (c)). For localized non-homogeneous B_m, the intensity of the contour falls rapidly with distance from the detector coil (figures 1(b) and (d)).

When a magnetic biosusceptometer, such as the one simulated in this work, is used to evaluate the iron concentration level in the liver, the contribution of the induced magnetism

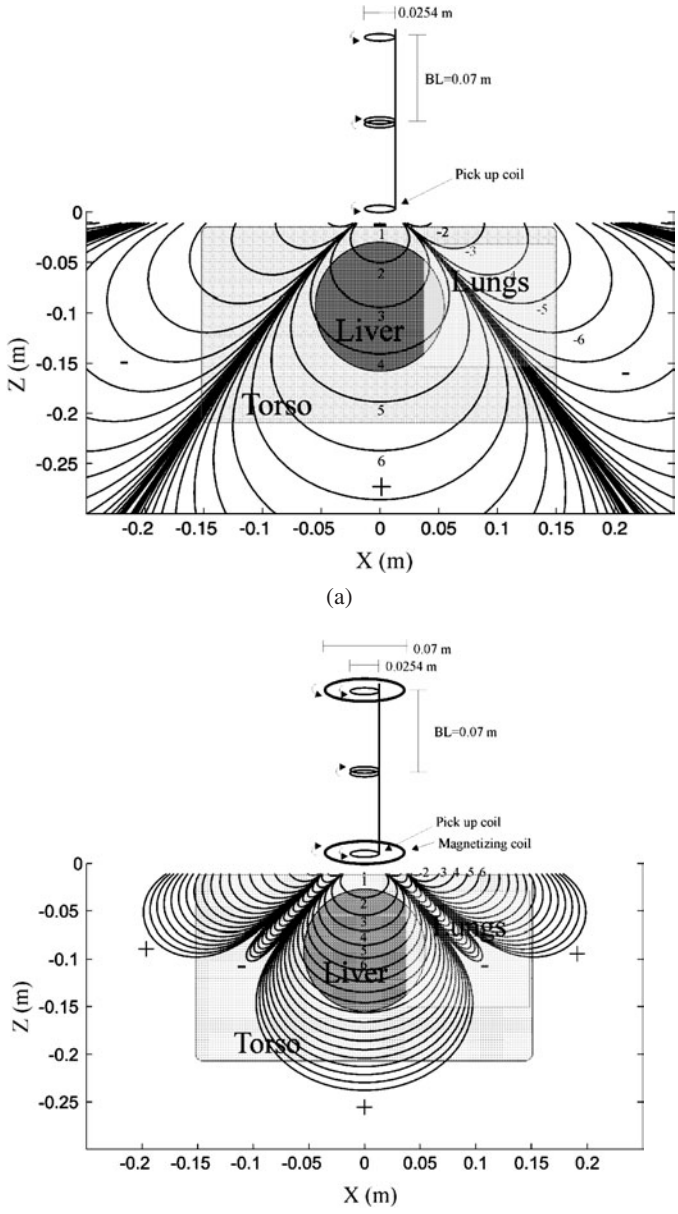

Figure 1. Calculated equal-sensitivity contours for a second-order axial gradiometer associated with a uniform axial field (a); a localized axial field (b); and for a first-order planar gradiometer associated with a uniform axial field (c); a localized axial field (d). These contours are mapped in a plane including the axis of the coil arrays and 0.01 m distant from the pick-up coil. The intensity of the contour n in the map is equal to $(\vec{B}_m \cdot \vec{B}_d)_{n=1}/n^5$. A projection of the torso and lung volumes with cylindrical geometry and liver volume with spherical geometry, with dimensions equivalent to an adult's organs, is superposed.

of each substance (tissue, iron, air, etc) and their position in relation to the detector are of paramount importance to get a good precision in the quantification of the liver iron. In a

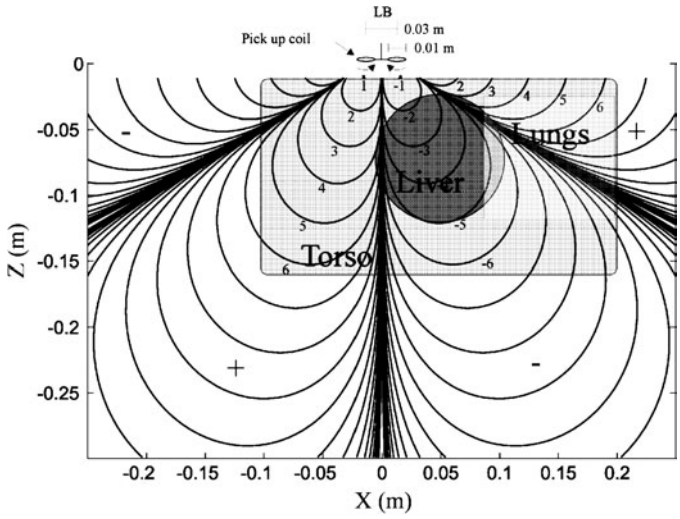

(c)

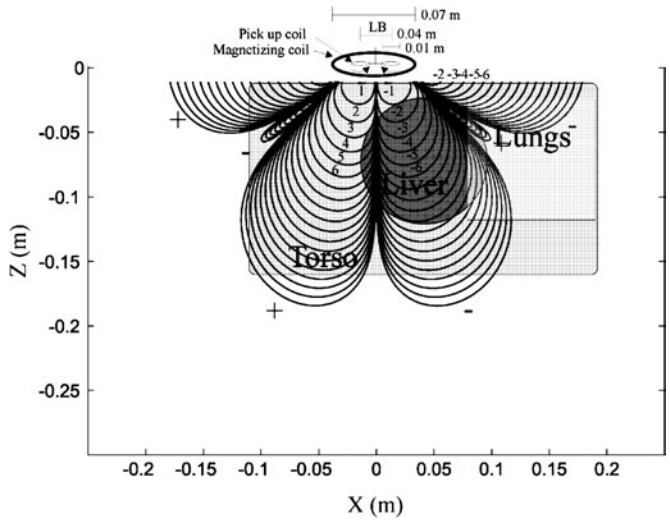

(d)

Figure 1. (Continued.)

susceptometric measurement of the liver, the torso is taken away from the pick-up coil during signal acquisition. In the simulation that follows, the initial position of the sample was 0.011 m from the detector and the final displacement was 0.111 m.

5. Equivalent LIC to some uncertainty in liver susceptometric measurement

Here we present an evaluation of the LIC corresponding to the estimated uncertainty in the position and size of the torso, liver and lung volumes during a hepatic iron susceptometric measurement. The results are expressed as the quantity of iron homogeneously distributed in

the liver volume that would produce the same intensity of susceptometric signal produced by each of the estimated uncertainties, i.e.

$$\delta c = [\chi_{\mathrm{VI}} \delta\, \mathrm{int}_{\mathrm{VI}}]/[\chi_{m,\mathrm{Fe}} \Delta \mathrm{int}_{\mathrm{liver}}] \tag{3}$$

where χ_{VI} is the volumetric susceptibility of the volume of interest; $\delta\, \mathrm{int}_{\mathrm{VI}}$ is the change in the value of the integral $\int_{\mathrm{VI}} B_m\,(r)\, \frac{B_d(r)}{I_d}\, \mathrm{d}r^3$, calculated over the volume of interest (VI), corresponding to each estimated uncertainty in the position and size of the VI, $\chi_{m,\mathrm{Fe}}$ is the mass susceptibility of the liver iron and $\Delta \mathrm{int}_{\mathrm{liver}}$ is the change in the value of the integral, calculated on the liver volume, when the torso is taken far from the pick-up coil (0.111 m in our simulation).

U1: Uncertainty in the initial position of the VI. This uncertainty is related to the positioning of the torso, the actual position of the lungs and liver inside the torso and, mainly, to the variation in the distance between the skin and the pick-up provoked by the breathing coil during a susceptometric measurement. The equivalent liver iron was evaluated independently for estimated uncertainty in the vertical (z) and horizontal (x, y) positions of each VI.

U2: Uncertainty in the estimation of the size of the VI. This uncertainty is related to the estimation of the dimensions of the VI, as well as the difference between the actual geometry of the VI and that attributed to resolve the integral of flux. For the cylindrical geometry attributed to the torso and lung volumes, the flux changes threading the detector coils are more dependent on the diameter than on the length of the cylinder. So, only the uncertainties in the diameter of the torso and the lung volumes were considered. To verify how much LIC corresponds to the uncertainty in the geometry of the liver, cylindrical and elliptical geometries instead of a spherical geometry for the liver volume, maintaining the same volume size, were considered. The quantity of LIC corresponding to this uncertainty was obtained using the following equation:

$$\delta c_{\mathrm{Fe}} = c_{\mathrm{Fe}} \left[\frac{\Delta \mathrm{int}_{\mathrm{liv,vol}}}{\Delta \mathrm{int}_{\mathrm{liv,sph}}} - 1 \right] \tag{4}$$

where c_{Fe} is the iron concentration in the liver, $\Delta \mathrm{int}_{\mathrm{liv,sph}}$ is the integral variation resolved on the spherical volume and $\Delta \mathrm{int}_{\mathrm{liv,vol}}$ is the integral variation solved on the cylindrical and elliptical volumes attributed to the liver. The quantity δc_{Fe} was also evaluated considering only the upper half of the VI for each geometry attributed to the liver.

For all simulated susceptometric systems, the considered magnetizing field was 1 mT on the upper surface of the liver when in the initial position (0.028 m from the pick-up coil). The mass susceptibility used for the hepatic iron was 1.600×10^{-6} m^3 kg^{-1} (SI) (the mass susceptibility of ferritin). The volumetric susceptibility used for the tissue was equal to that of water (-9.032×10^{-6} (SI)) and 0.36×10^{-6} (SI) for the air in the lungs.

6. Results and discussions

The magnetic flux threading the detector coil, due to the presence of the normal iron concentration (300 μg Fe/g$_{\mathrm{wet\ tissue}}$) homogeneously distributed in the liver volume and lung air volume was evaluated independently for different detector–skin distances, for the four susceptometric systems described in this work (figure 2). It was obtained using equation (2). Tables 1 and 2 show the calculated iron concentration (δc_{Fe}) corresponding to the estimated uncertainty in analysed parameters present in a susceptometric measurement, obtained using equation (3). The uncertainties due to the presence of the tissue layers were evaluated without the water bag.

The magnetic flux threading the second-order axial and first-order planar gradiometer detectors for a susceptometric measurement of the hepatic iron when magnetized with

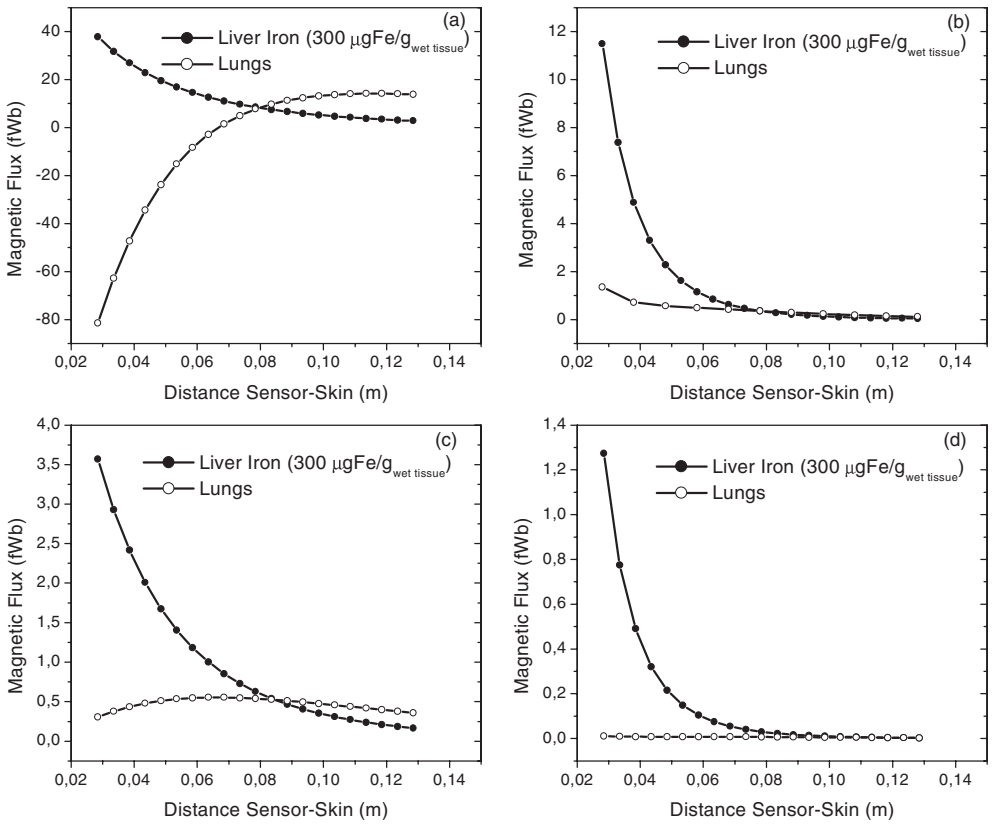

Figure 2. The magnetic flux threading the detector coils, due to the presence of the normal iron concentration (300 mg $Fe/g_{wet\ tissue}$) homogeneously distributed in the liver volume and lung air volume, evaluated independently for different detector–skin distances, for the four susceptometric configurations presented in figure 1: (a) HMF + SOAG; (b) LMF + SOAG; (c) HMF + FOPG; (d) LMF + FOPG.

homogeneous and local fields were shown. When a HMF is used the entire sample is homogeneously magnetized, so the sensitivity contours depend only on the geometry of the detector coil. When a non-HMF is used, the sensitivity contours depend on the association of the magnetizing coil with the detector coil, being highest for a small volume near the pick-up coil. Therefore, in a hepatic susceptometric measurement using a LMF, the portion of the liver that contributes to the signal is smaller than when using a HMF.

Certainly, a good strategy to reduce the stronger variation in the susceptometric signal coming from the intervening tissue is to fill all the free space between the magnetic detector and the torso with water. But, according to the map of equal sensitivity (figure 1), except for a susceptometer using a SOAG detector together with a LMF, this variation in the signal coming from the tissue can also be minimized just by regularizing the upper surface of the torso with water or other substance with similar susceptibility instead of filling all the free space between the magnetic detector and the torso with water. It is possible for this detector coil configuration, because part of the volume of the torso that contributes positively to the magnetic flux is equivalent to that contributing negatively. Although, the uncertainty in the hepatic iron level equivalent to the parameters of the tissue volume was practically null when

Table 1. Uncertainty of the hepatic iron concentration determination corresponding to the estimated uncertainty in the parameters present in the susceptometric measurement of the liver evaluated for the four simulated susceptometer systems.

		Uncertainty of hepatic iron (δc_{Fe}) (μg Fe/g$_{wet\ tissue}$)			
		HMF		LMH	
VI	Parameter uncertainty	SOAG	FOPG	SOAG	FOPG
Tissue	Vertical position (δz_{torso}) = 0.003 m	412	30	7830	3
	Horizontal position (δx_{torso}) = 0.01 m	115	100	1030	8
	Cylindrical radius ($\delta \rho_{torso}$) = 0.01 m	298	90	37	1
Lungs	Vertical position (δz_{lung}) = 0.003 m	98	38	7	2
	Horizontal position (δi_{lung}) = 0.01 m	40	144	5	10
	Cylindrical radius ($\delta \rho_{lung}$) = 0.01 m	80	96	3	20
Liver	Vertical position (δz_{liver}) = 0.003 m	0.090 c_{ftn}	0.115 c_{ftn}	0.770 c_{ftn}	0.240 c_{ftn}
	Horizontal position (δr_{liver}) = 0.01 m	0.053 c_{ftn}	0.044 c_{ftn}	0.074 c_{ftn}	0.242 c_{ftn}
	Spherical radius ($\delta \rho_{liver}$) = 0.01 m	0.068 c_{ftn}	0.017 c_{ftn}	0.030 c_{ftn}	0.015 c_{ftn}

Table 2. Uncertainty of the hepatic iron concentration determination using a magnetic susceptometry method corresponding to the estimated uncertainty in the geometry of the volume of the liver evaluated for the four simulated susceptometer systems.

		Uncertainty of hepatic iron/ hepatic iron level ($\delta c_{Fe}/c_{Fe}$)			
		HMF		LMF	
Liver geometry	Dimension	SOAG	FOPG	SOAG	FOPG
Spherical	$r = 0.071$ m	0	0	0	0
Half spherical	$r = 0.071$ m	0.141	0.110	0.110	0.016
Elliptical	$a = 0.100$ m; $b = 0.070$ m; $c = 0.050$ m	0.095	0.017	0.051	0.003
Half elliptical	$a = 0.100$ m; $b = 0.070$ m; $c = 0.050$ m	0.371	0.175	0.013	0.123
Cylindrical	$r = 0.07$ m; $l = 0.095$ m	0.007	0.133	0.056	0.128
Half cylindrical	$r = 0.07$ m; $l = 0.095$ m	0.151	0.044	0.042	0.118

a FOPG detector is used, in a real measurement in humans, it is not true due to the irregularity in the upper surface of the torso from one person to another.

When the torso is moved away from the pick-up coil the magnetic flux threading the detector coils derived from the lung volumes is equivalent to the magnetic flux derived from the normal level of iron in the liver when the torso is magnetized with a HMF. On the other hand, the susceptometric perturbation of the lung is practically null when a LMF is used (figure 2).

The large uncertainty in the measurement of the hepatic iron concentration caused by the presence of the tissue, when using a SOAG (table 1), shows why the use of the water is necessary to fill the space between the detector and the torso to minimize the tissue perturbation.

According to tables 1 and 2, the uncertainties in the hepatic iron quantification, using one of these susceptometric configurations, are not critical to the considered uncertainties in the size and geometry of liver volume. Obviously, the larger the liver iron level, the larger this uncertainty would be. The uncertainty in the hepatic iron quantification corresponding to

the small displacement in the vertical distance detector–liver is considerably high for all four systems, being higher when a non-homogeneous magnetizing field is used.

According to the results presented, all the configurations of the superconductor susceptometer simulated have the potential to evaluate the level of hepatic iron, however with some instrumental and/or practical limitations.

The great advantage of using a LMF instead of a HMF is that the first can be applied with a superconducting coil and be associated with detector coils in the same substrate support inside the dewar, allowing a higher magnetizing field and lower noise (Paulson *et al* 1990). On the other hand, for large samples such as the liver, the sensitivity of a susceptometer with this kind of magnetization is practically due to the small portion of the sample nearest to the pick-up coil. Consequently, the susceptometric measurement is very critical with regard to a distance between the sample and the pick-up coil. The application of HMF is generally made using larger coils, therefore, it is more difficult to apply a high intensity (>0.2 mT) magnetizing field. However, the use of a lock-in detection technique associated with low intensity ac external fields endows the instrument with sensitivities comparable with dc magnetizing field systems (Bastusheck and Williamson 1985, Carneiro and Baffa 2000). In practical terms, the use of a FOPG makes the susceptometer less sensitive to large samples such as the liver. Figure 2 shows that the magnetic flux threading this detector coil was ten times less sensitive than using a SOAG. Other configurations for the magnetizing system could increase the sensitivity of the susceptometer with a FOPG (Della Pena *et al* 1999).

In conclusion, the critical parameters for precise determination of iron concentration in the liver were discussed. Strategies to keep the important parameters under control can be devised. At present, both homogeneous and non-homogeneous magnetizing field susceptometers are employed in iron overload measurements. It is possible that with the refinement of modelling iron deficiency could also be assessed by susceptometric measurements.

References

Baffa O, Tannus A, Zago M A, Figueiredo M S and Panepucci H C 1986 Changes in NMR relaxation times of iron overloaded mouse tissue *Bull. Magn. Reson.* **8** 69–73

Bastuscheck C M and Williamson S J 1985 Technique for measuring the ac susceptibility of portions of the human body or other large objects *J. Appl. Phys.* **58** 3896–906

Brittenham G M, Farrel D E, Harris J W, Feldman E S, Danish E H, Muir W A, Tripp J H, Brennan J N and Bellon E M 1982 Diagnostic by magnetic suscetibility measurement assessment of human iron stores *N. Engl. J. Med.* **307** 1671–5

Carneiro A A O and Baffa O 2000 Susceptometric measurement of liver *in vivo* using a AC homogenous magnetizing field *Advances in Biomagnetism: Proc. 12th Int. Conf. on Biomagnetism*

Clark P R and St. Pierre T G 2000 Quantitative mapping of transverse relaxivity ($1/T_2$) in hepatic iron overload: a single spin-echo imaging methodology *Magn. Reson. Imaging* **18** 431–8

Della Penna S, Del Gratta C, Di Luzio S, Pizzella V, Torquati K and Romani G L 1999 The use of an inhomogeneous applied field improves the spatial sensitivity profile of an *in vivo* SQUID susceptometer *Phys. Med. Biol.* **44** N21–9

Engelhardt R, Langkowski J H, Fischer R, Nielsen P, Kooijman H, Heinrich H C and Bücheler E 1994 Liver iron quantification: studies in aqueous iron solutions, iron overloaded rats and patients with hereditary hemochromatosis *Magn. Reson. Imaging* **12** 999–1007

Farrel D E, Tripp J H, Brittenham G M, Danish E H, Harris J W and Tracht A E 1983 A clinical system for accurate assessement of tissue iron concentration *Lett. Nuovo Cimento* **2** 582–93

Farrel D E, Tripp J H, Zanzucchi P E, Harris J W, Brittenham G M and Muir W A 1980 Magnetic measurement of human iron stores *IEEE Trans. Magn.* **16** 818–23

Fischer R, Engelhardt R, Nielson P, Gabbe E E, Eich E, Heinrich H C, Schmiegel W H and Wurbs D 1992 Liver iron quantification in the diagnosis and therapy control of iron overload patients *Biomagnetism: Clinical Aspects, Proc. 8th Int. Conf. on Biomagnetism* (Amsterdam: Elsevier) pp 585–8

Gomori J *et al* 1991 Hepatic iron overload: quantitative MR imaging *Radiology* **179** 367–8

Jensen P D, Jensen F T, Christensen T and Ellergaard J 1994 Non-invasive assessment of tissue iron overload in the liver by magnetic resonance imaging *Br. J. Haematol*. **87** 171–84

Kaltvasser J P, Gottschalk R, Schalk K P and Hartl W 1990 Non-invasive quantification of liver iron-overload by magnetic resonance imaging *Br. J. Haematol*. **74** 360–3

Papakonstantinou O G. *et al* 1995 Assessment of liver iron overload by T2-quantitative magnetic resonance imaging: correlation of T2-QMRI measurements with serum ferritin concentration and histologic grading of siderosis *Magn. Reson. Imaging* **13** 967–77

Pasquarelli A, Del Gratta C, Della Penna S, Di Luzio S and Pizzella V 1996 A SQUID based AC susceptometer for the investigation of large samples *Phys. Med. Biol*. **41** 2533–9

Paulson D N, Fagaly R L and Toussaint R M 1990 Biomagnetic susceptometer with SQUID instrumentation *IEEE Trans. Magn.* **27** 3249–52

Thomsen C, Wiggers P, Ring-Larsen H, Christiansen E, Dalhoj J, Henriksen O and Christoffersen P 1992 Identification of patients with hereditary haemochromatosis by magnetic resonance imaging and spectroscopic relaxation time measurements *Magn. Reson. Imaging* **10** 867–79

Tripp J H 1983 Biomagnetism: an interdisciplinary approach *Physical Concepts and Mathematical Models* ed S J Williamson, G L Romani, L Kaufman and I Modena (New York: Plenum) pp 101–39